Efficient and poison-tolerant Pd$_x$Au$_y$/C binary electrocatalysts for glucose electrooxidation in alkaline medium

Longlong Yan [a], Angeliki Brouzgou [b], Yuezhong Meng [a], Min Xiao [a,***],
Panagiotis Tsiakaras [b,**], Shuqin Song [a,*]

[a] State Key Laboratory of Optoelectronic Materials and Technologies/The Key Lab of Low-carbon Chemistry & Energy Conservation of Guangdong Province,
School of Physics and Engineering, Sun Yat-sen University, Guangzhou 510275, China
[b] Department of Mechanical Engineering, School of Engineering, University of Thessaly, Pedion Areos 38834, Greece

ARTICLE INFO

ABSTRACT

Carbon supported Pd$_x$Au$_y$ binary catalysts for glucose electrooxidation and detection were prepared by a modified pulse microwave assisted polyol method. The physico-chemical properties were obtained by X-ray diffraction (XRD), transmission electron microscopy (TEM) and scanning electron microscopy with energy-dispersive X-ray spectroscopy (SEM-EDS). The electrochemical activity was investigated through cyclic voltammetry and chronoamperometry. Based on the experimental results, it can be concluded that the combination of Pd and Au to get Pd$_x$Au$_y$ binary catalysts can take advantage of the high activity and low overpotential of Pd to glucose electrooxidation and poison tolerance of Au. More precisely, when the Pd/Au molar ratio was 30:70 (Pd$_{30}$Au$_{70}$/C), a desirable comprehensive performance, considering from current density, overpotential, and poison tolerance ability, was obtained. It was also found that Pd$_{30}$Au$_{70}$/C exhibited a very sensitive and linear amperometric response for glucose molecules, promising for the development of electrochemical glucose sensors and direct glucose fuel cells.

1. Introduction

Glucose electrooxidation has been the hot research topic in electrochemistry due to the importance of reliable and fast *in vivo* or *in vitro* monitoring of blood sugar for the treatment and control of diabetes through an electrochemical glucose sensor, as well as the interest for implantable glucose fuel cells intended for artificial hearts and heart pacer [1–8]. However, their research and development is far away from satisfaction and real applications for lack of highly efficient and stable electrocatalysts for glucose electrooxidation. Desirable electrocatalysts, reflected in terms of high current and low overpotential for glucose oxidation and good poison tolerance, is the solution to achieve fast response for glucose detection and high performance for direct glucose fuel cells. At present, Pt [9–11], Au [12–18], Pd [19–21] and their based binary or ternary catalysts such as PtPd [5,22,23], PtBi [24], PtRu [24], PtPb [25,26], PtAu [22,24,27–30], AuAg [31], PtAuPd [5], *etc.*, and muti-wall carbon nanotubes [32] have been found to exhibit electrocatalytic activity to glucose oxidation. Very recently we have reported that

PdRh/C electrocatalyst [33] exhibited very good performance to glucose electrooxidation, suggesting it is a plausible anode material for direct glucose fuel cells. Among them, Pt is the first discovered and widely investigated material. But Pt is not a very suitable one due to its high chemisorbability for different substances present in physiological solutions and its poor selectivity in the presence of various organic substances [12]. Au has also been extensively studied for glucose electrooxidation in alkaline solution since its first report [34] and exceeds Pt in its electrocatalytic activity and poison tolerance to glucose oxidation in neutral and alkaline solutions. However, the potential for glucose oxidation at Au is still too high for glucose detection [35]. Alloy electrocatalysts are often adopted to obtain better performance than pure metals through exploiting the specific properties of each component [36–38]. It has been recognized that the activity of Pt to glucose electrooxidation in alkaline media can be enhanced by alloying Pd, Au, Bi, Ru, *etc.* [5,22–29]. On the other hand, the novel efficient and stable electrocatalysts for glucose electrooxidation are still urgently needed.

Pd has been known to exhibit superior activity for the electrooxidation of alcohols and polyalcohols in alkaline solutions [39]. Furthermore, the abundance of Pd on the earth is at least 50 times more than that of Pt. The combination of Pd and Au has exhibited good catalytic activity to glucose selective oxidation [40]. However, for the electrochemical oxidation of glucose at PdAu, to our best knowledge, there is no systematic investigation. In the present work, a series of Pd$_x$Au$_y$/C catalysts with different

* Corresponding author. Tel.: +86 20 84113253; fax: +86 20 84113253.
** Corresponding author. Tel.: +30 24210 74065; fax: +30 24210 74050.
*** Corresponding author. Tel.: +86 20 84115506; fax: +86 20 84114113.
    E-mail addresses: stsxm@mail.sysu.edu.cn (M. Xiao), tsiak@uth.gr (P. Tsiakaras),
stsssq@mail.sysu.edu.cn (S. Song).

Pd/Au molar ratios were prepared by the modified pulse microwave assisted polyol synthesis method in a very short time (2 min). Their corresponding physico-chemical characteristics were obtained by X-ray diffraction (XRD), transmission electron microscopy (TEM), and scanning electron microscopy-energy dispersive spectroscopy (SEM-EDS). The electrocatalytic activity to glucose electrooxidation was evaluated by the electrochemical methods including cyclic voltammetry (CV), chronoamperometry (CA) in the alkaline environment in the absence or presence of glucose.

2. Experimental

2.1. Materials

Carbon black (Vulcan XC-72R, Cabot Corp.), $PdCl_2$ (Guiyanboye Corp., AR), $HAuCl_4 \cdot 4H_2O$ (Guiyanboye Corp., AR), ethylene glycol (Shanghailingfeng Corp., AR), Nafion (DuPont, 5 wt.%) were used without further purification. All other chemicals used are of analytical reagent grade. High quality deionized water (resistivity > 18.0 MΩ cm^{-1}) used for all experiments was prepared by a water purification system.

2.2. Catalyst preparation

Vulcan XC-72R carbon black supported Pd_xAu_y (x and y denote the respective molar ratio for Pd and Au) binary catalysts with 20 wt.% noble metal were prepared by a modified microwave assisted polyol method [41,42]. A certain amount of $PdCl_2$/ethyl glycol (EG) or/and $HAuCl_4$/EG solution was well mixed with EG in an ultrasonic bath, and then carbon black powder was added into the solution according to the pre-calculated metal loading. After stirring, 2.0 mol L^{-1} NaOH/EG was added into the solution to adjust the pH value of the above mixture to be more than 12. After further stirring for another 1 h, the slurry was microwave-heated (Nanjinghuiyan Corp., MZG800S) for several times in a 10 s-on/10 s-off pulse form and then re-acidified. The obtained black solid sample was washed by hot deionized water and dried in a vacuum oven at 80 °C for 12 h.

2.3. Chemico-physical characterization

The XRD patterns were recorded on a D-MAX 2200 VPC diffractometer using Cu Kα radiation (30 kV, 30 mA). TEM investigations were carried out on a JEOL TEM-2010 (HR) to determine the size and surface morphology of the catalyst particles. Before the measurements, the catalysts were uniformly dispersed in ethanol solution using an ultrasonic water bath and then dried onto carbon coated copper grid. For the determination of metal content in the catalysts, thermogravimetric (TG) experiments were carried out with a Netzsch TG-209 analyzer in air with a flow rate of 50 mL min^{-1} and a temperature ramp of 10 °C min^{-1}. The SEM-EDS was performed on scanning electron microscope (JEOL JSM-6330F) to determine the chemical composition of the samples.

2.4. Electrochemical analysis

Three-electrode electrolytic cell was used to perform the electrochemical evaluation on an AUT84480 instrument in a thermostatic water bath. Platinum foil (1.0 cm × 1.0 cm) and Hg/HgO electrode (1 mol L^{-1} KOH) were used as the counter and reference electrodes respectively. The catalyst thin film was covered onto the surface of the glassy carbon disk electrode (d = 0.5 cm), which was used as the working electrode. The catalyst slurry was obtained by dispersing 5.0 mg of the as-prepared catalyst powder in 1.8 mL ethanol and 0.2 mL Nafion solution. The above obtained catalyst ink was then quantitatively (10 μL) transferred onto the surface of the glassy carbon electrode and dried in an infrared lamp. The CV and CA techniques were adopted to evaluate and compare the electrocatalytic performance of the catalysts for glucose electrooxidation in alkaline medium. Before experiments, the solution was saturated with high-purity N_2 gas for 30 min to remove the dissolved oxygen in the electrolyte. It should be noted that the potential is referred to Hg/HgO (1 mol L^{-1} KOH) reference electrode without specification.

3. Results and discussion

3.1. Physico-chemical characterization

XRD patterns for all the as-prepared Pd/C, Au/C, and Pd_xAu_y/C samples are displayed in Fig. 1. All the catalysts give a broad peak at about $2\theta = 25°$ assigned to graphitic carbon (0 0 2). Moreover, all the samples present a typical fcc pattern. By comparing Figs. 1A and B, one can distinguish that for single metals the diffraction peaks do not coincide as the corresponding diffraction angles of Au/C is a little higher than those of Pd/C (Fig. 1A), while the diffraction peaks for Pd and Au are overlapped and cannot be obviously differentiated (Fig. 1B). However, in the fine scanning from 62 to 70° at 1° min^{-1}, the diffraction peaks for Au (3 1 1) and Pd (3 1 1) can be distinguished. This could indicate that there are some interactions between Pd and Au in Pd_xAu_y/C binary catalysts. But PdAu alloy was not formed due to the low temperature for catalysts preparation process (<160 °C). Whereas, in the case of $Pd_{90}Au_{10}$/C and $Pd_{70}Au_{30}$/C, the Au (3 1 1) diffraction peak is not detected, which is probably due to the low content of Au. Table 1 lists the crystallite sizes calculated from the Pd (2 2 0) or Au (2 2 0) diffraction peak using the Scherrer formula [43]. It can be clearly seen from Table 1 that the crystallite size of mono metallic catalyst is bigger than that of binary ones. The further decrease in the particle size of the catalyst could give higher activity, and this part work is under investigation.

Fig. 2 depicts the typical TEM images for Pd/C, Au/C, $Pd_{70}Au_{30}$/C and $Pd_{30}Au_{70}$/C and their corresponding metal particle size distribution. Obviously, Pd/C has a smaller particle size and better dispersion than Au/C. For binary catalysts, the metal particle size becomes smaller than that of the single metal. These results agree with those of XRD, although the calculated crystallite size from XRD is bigger than the statistical value from TEM.

The metal content in the catalysts is a very important parameter for comparing the activity of different catalysts. So, the metal content in Pd/C and Au/C was determined by TG to check what extent the metal precursors can be reduced. As shown in Fig. 3, below 200 °C, the weight loss for two samples can be attributed to the desorption of water vapor and the residual EG. Therefore, the metal loading in the electrocatalysts can be calculated from their TG curves after subtracting the weight of adsorbed water and the results are summarized in Table 1. It should be noted that Pd and Au was adopted for the residual materials after TG test, which has been confirmed by the XRD results (inset of Fig. 3) of the heat-treatment under the same operation conditions of TG results. Setting the weight of the anhydrous material to 100 wt.%, the metal loading in all the catalysts is 20.0 ± 1.5 wt.%, which is basically in accordance with the feeding weight ratio (20.0 wt.%) for catalysts preparation. This indicates that the pulse-microwave assisted polyol synthesis method adopted in the present work is an effective and fast one for both Pd and Au catalysts. The Pd/Au molar ratio in the Pd_xAu_y/C binary catalysts can be determined from SEM-EDS (Fig. S1) and summarized in Table 1. The results show that the final Pd/Au molar ratio is close to the feeding ratio in the precursor solution.
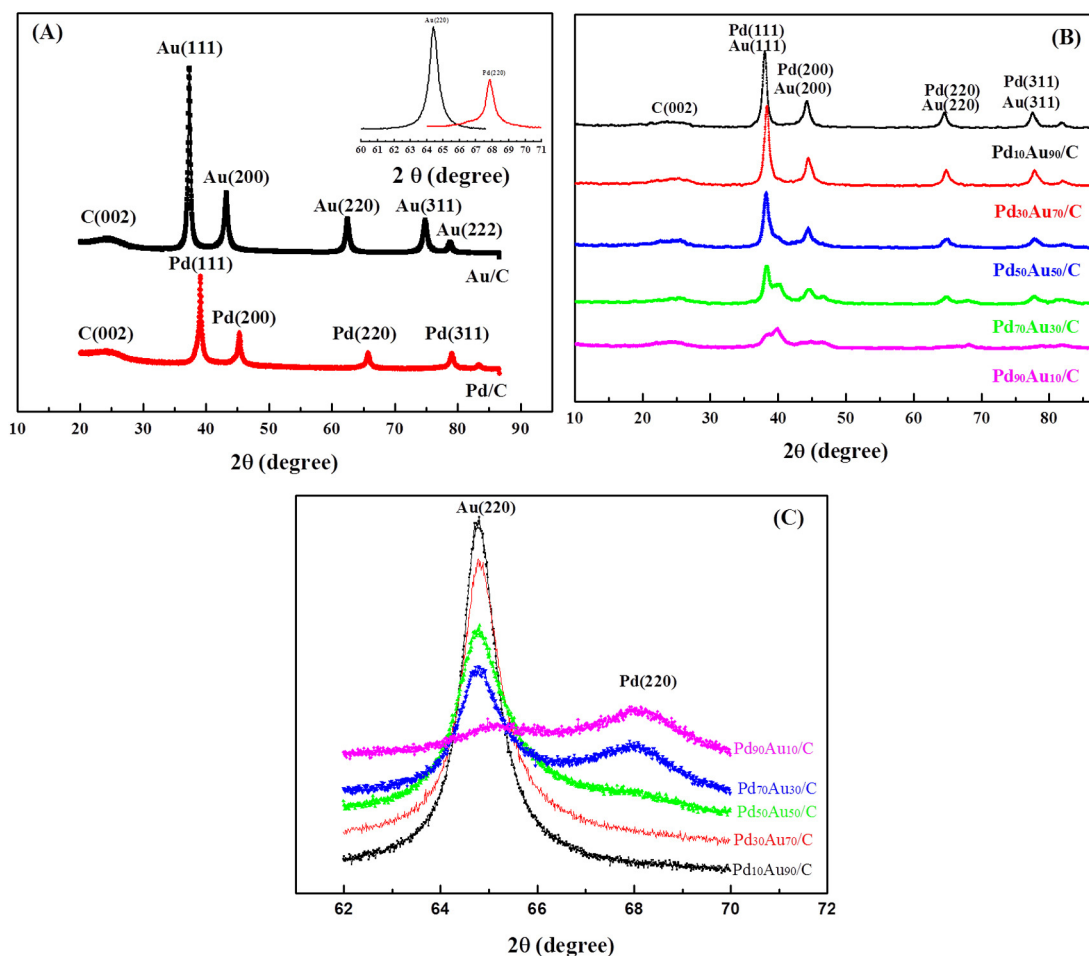
Fig. 1. XRD patterns for Pd/C and Au/C (A) and Pd_xAu_y/C binary catalysts (B) and their corresponding detailed Pd or Au (2 2 0) peaks scanned at 1° min^{-1} (C).

Table 1
Physico-chemical properties of the as-prepared Pd/C, Au/C and Pd_xAu_y/C catalysts.

Samples	Crystallite size/nm	Mean particle size/nm	Pd/Au atomic ratio		Metal content (wt.%) (TG)
	XRD	TEM	EDS	Feeding ratio	
Pd/C	12.6	8.1	–	–	19.2
$Pd_{90}Au_{10}$/C	9.7	–	88.4/11.6	90/10	21.3
$Pd_{70}Au_{30}$/C	8.1	4.9	77.0/23.0	70/30	22.1
$Pd_{50}Au_{50}$/C	7.3	–	53.3/46.7	50/50	19.7
$Pd_{30}Au_{70}$/C	7.1	4.8	24.5/75.5	30/70	18.5
$Pd_{10}Au_{90}$/C	6.6	–	7.6/92.4	10/90	19.5
Au/C	16.2	14.0	–	–	20.8

3.2. Electrochemical characterization

The electrocatalytic activities of the as-prepared catalysts toward glucose electrooxidation were evaluated through potentiodynamic voltammetric curves. The polarization curves for Pd/C and Au/C mono-metallic catalysts in 0.1 mol L^{-1} NaOH solution in absence or presence of 20 mmol L^{-1} glucose are given in Fig. 4. For Pd/C catalyst (Fig. 4A), the disappearance of hydrogen desorption peak in the presence of glucose indicates the adsorption of glucose at Pd hinders the adsorption of hydrogen. An obvious maximum peak (P_{af}) can be discerned in the forward direction, which corresponds to the direct glucose oxidation after the poisoning intermediates on the electrocatalyst surface are moved by the OH$_{ad}$ radicals formed by the partial discharge of OH$_{ad}$ under the upper potential region [44,45]. After the maximum, the current decreases sharply due to the formation of palladium oxidation at this potential. In the backwards direction, the reduction peak (P_{cb}) is attributed to the reduction of PdO and the oxidation peak (P_{ab}) is formed through the direct glucose oxidation at Pd reduced from PdO. The further comparison of polarization curve of glucose electrooxidation at Pd/C with the potentiodynamic curve of Pd/C in the blank solution shows that the reduction peak of PdO is obviously decreased in the former case. This suggests part of Pd has been poisoned during the electrooxidation of glucose. For Au/C catalysts (Fig. 4B), in the forward direction, the observed first oxidation peak (P_{af1}) is probably due to the formation of Au(OH)$^{1-\lambda}$ and the adsorption of glucose [15,46]. The other two significant oxidation peaks (P_{af2} in forward direction and P_{ab} in the backward direction) is the electrooxidation of glucose at gold hydroxide. Furthermore, the close peak current density of P_{af2} and P_{ab} gives an indicator that Au is tolerant to the intermediate products of glucose oxidation. By comparing the CV curves at Au/C in 0.1 mol L^{-1} NaOH in the
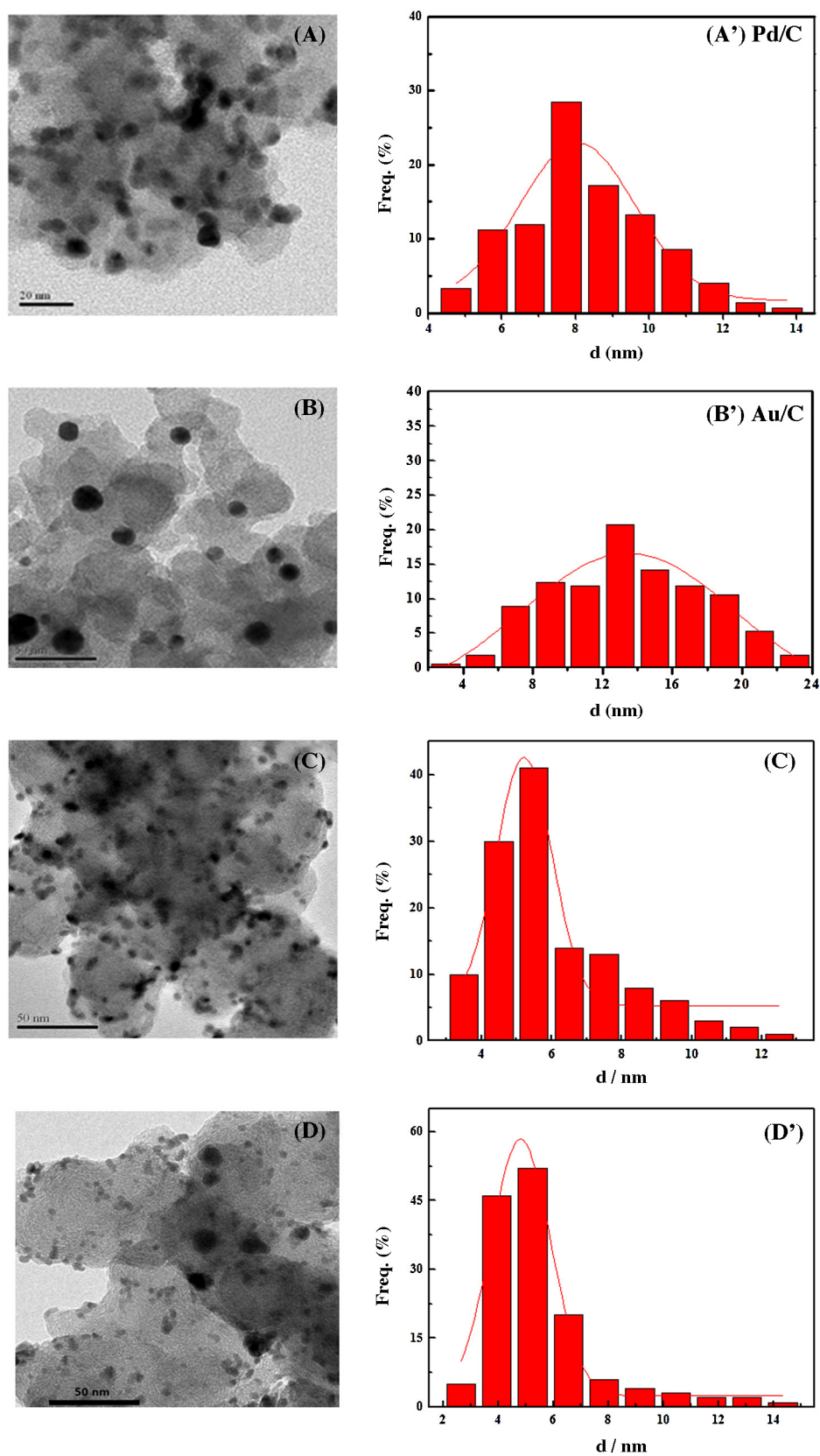
Fig. 2. TEM images of Pd/C (A), Au/C (B), $Pd_{70}Au_{30}$/C (C) and $Pd_{30}Au_{70}$/C (D) and their corresponding particle size distribution (A′, B′, C′ and D′).
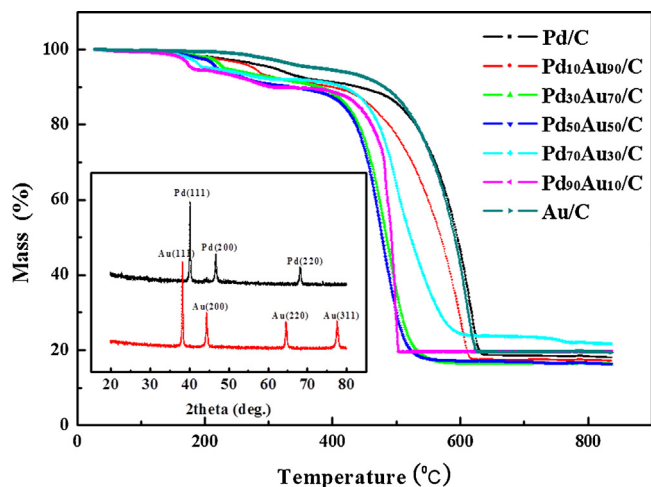
Fig. 3. Thermogravimetric curves of Pd/C, Au/C and Pd_xAu_y/C samples.

Fig. 5. Comparative results of glucose electrooxidation at Pd/C and Au/C. Electrolyte: 0.1 mol L^{-1} NaOH + 20 mmol L^{-1} glucose; scan rate: 50 mV s^{-1}, temperature: 36.5 °C.

absence or presence of glucose, it can be distinguished that glucose electrooxidation starts long before the noticeable oxidation of gold begins.

The polarization curves of glucose electrooxidation at Pd/C and Au/C are compared in Fig. 5. As clearly shown, from the point of view of current density, Pd/C gives a little higher activity than Au/C in the forward potential scanning, while in the backward direction, Au/C exhibits superior performance. On the other hand, considering from the overpotential point view, Pd/C has an obvious advantage over Au/C. Including also the above discussions of poison sensitivity of Pd/C while good poison tolerance of Au/C during glucose electrooxidation, the combination of Pd and Au is expecting to be the solution for active and poison tolerant catalysts.

In background solution (0.1 mol L^{-1} NaOH), the potentiodynamic curves at Pd/C, Au/C and Pd_xAu_y/C mono or binary catalysts are shown in Fig. 6A. As it is observed the formation of surface oxides at potential values more positive than −0.15 V and the reduction of surface oxides in the cathodic potential scan take place. The as-reported catalytic oxides, AuOH and PdOH, can be attributed to the chemisorption of hydroxide ions onto catalyst's surface. From the potential range of the surface oxide formation it can be seen that the value of the potential of the surface oxide formation region lowers as the Au content increases, suggesting that the electrode is more stable. During the cathodic scan, the red-colored peak (P_{R1}) is attributed to the reduction of gold oxide species, while the
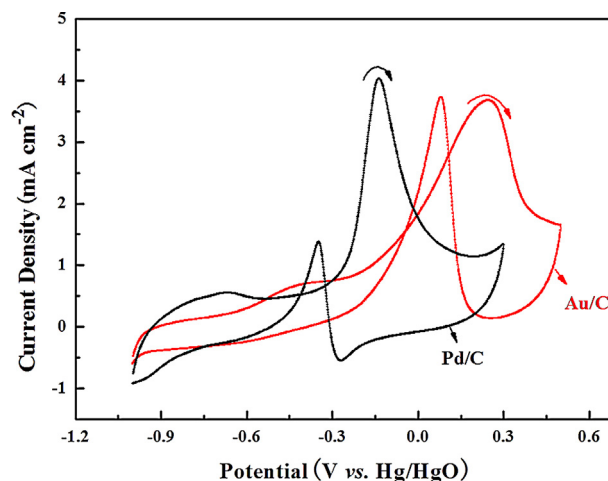
black-colored peak (P_{R2}) is attributed to the reduction of palladium oxide species. Moreover, a reduction peak potential difference that can be seen indicates the potential difference in the formation of the monolayer oxide during the anodic sweep. Clearly, along with the Au content increment in the catalysts, the peak area of P_{R1} is increased while that of P_{R2} is decreased, indicating how Au can positively contribute to the low number of metal oxides.

This indicates that Pd_xAu_y/C binary catalysts have been successfully synthesized, which agrees with the SEM-EDS results as shown in Fig. S1. Their electrocatalytic activities were obtained in 0.1 mol L^{-1} NaOH aqueous solution containing 20 mmol L^{-1} glucose. As shown in Fig. 6B, the samples with high Pd content (Pd/C, $Pd_{90}Au_{10}$/C, $Pd_{70}Au_{30}$/C, and $Pd_{50}Au_{50}$/C) exhibit two visible oxidation peaks in the forward sweep and an oxidation peak and a reduction peak in the backward sweep. While for the samples with low Pd content (Au/C, $Pd_{30}Au_{70}$/C, and $Pd_{10}Au_{90}$/C), the reduction peak in the backward sweep disappears. With the Pd content decrement, the first oxidation peak current in the forward sweep is decreased.

The first oxidation peak during the anodic scanning can be attributed to the formation of catalytically active sites Pd-OH$_{ads}$ or Au-OH$_{ads}$ which is the most important step for glucose oxidation. The second oxidation peak at potential values higher than 0.3 V may be due to either a surface reaction of Pd(OH) or PdO with the solution phase glucose or a further oxidation of an adsorbed species at
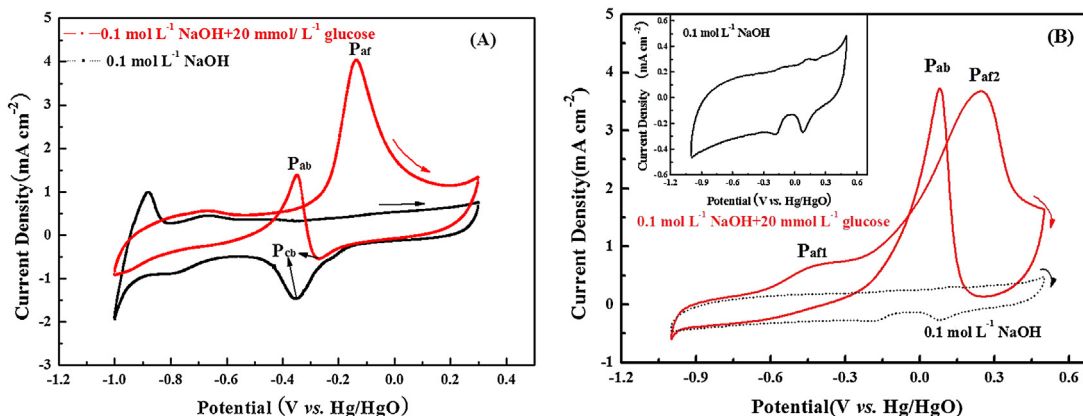

Fig. 4. Cyclic voltammetric curves of Pd/C (A) and Au/C (B) in 0.1 mol L^{-1} NaOH aqueous solution in the absence or presence of 20 mmol L^{-1} glucose at 50 mV s^{-1} and at 36.5 °C.
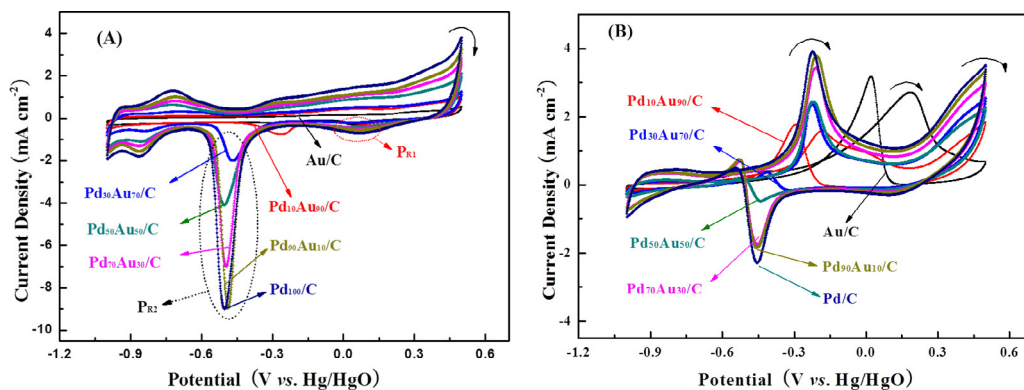
Fig. 6. Cyclic voltammetric curves of Pd/C, Au/C and Pd_xAu_y/C mono and binary catalysts in 0.1 mol L^{-1} NaOH aqueous solution in the absence (A) or presence of 20 mmol L^{-1} glucose (B) at 50 mV s^{-1} and at 36.5 °C.

more anodic potential. Additionally, the presence of another oxidation peak during the backward scanning may suggest that glucose's quick formed intermediates or fresh glucose are further oxidized. On the other hand the reduction peak is mainly ascribed to the reduction of metal oxides to their metal form [47].

However, the mechanism of the glucose oxidation in alkaline solution appears to be very complex, thus its elucidation requires a combination of electrochemical and separation methods as well as further investigation [47].

Furthermore, one can distinguish that the introduction of Au into Pd/C catalyst almost does not change the onset potential of glucose oxidation. Moreover, as the Au content increases, the oxidation peak current in the backward sweep increases and the corresponding peak potentials are obviously more positive. More precisely, the $Pd_{10}Au_{90}$/C sample exhibits very high oxidation peak (backward scan), indicating that glucose oxidation can be facilitated at this catalyst, however its lower peak current density during forward scan does not make it a good candidate for further investigation. This indicates the introduction of Au increases the poison tolerance of Pd to the intermediate products of glucose oxidation. Considering the activity and poison-tolerance together, $Pd_{30}Au_{70}$/C is chosen for the further investigation.

Fig. 7 shows the cyclic voltammetric curves at $Pd_{30}Au_{70}$/C in different concentrations of glucose while a constant concentration of NaOH (0.1 mol L^{-1}). From Fig. 7A, obviously, as the glucose concentration increases, the response current density linearly increases and arrives at about 3.0 mA cm^{-2} for 50 mmol L^{-1} glucose. This

performance enhancement could be attributed to the more reactants involved in the reaction as the glucose concentration is increased. On the other hand, the further increase in the glucose concentration causes the corresponding current density to linearly decrease as shown in Fig. 7B. This deteriorated performance could be due to the following reasons: (i) the given electrode surface cannot provide sufficient active sites for the electrocatalytic process, which leads to the ineffectiveness of higher concentration of glucose; (ii) higher concentration of glucose gives rise to higher viscosity of the solution, and thus more difficult mass transfer; and (iii) the byproducts may also cover the electrode surface to decrease its catalytic activity. This tendency agrees well with the reported results [16].

For the application of chemical sensor, electrocatalysts are generally evaluated by monitoring the current response along with time at a fixed potential after addition of the analyte and possible interfering agents [48,49]. In order to detect the actual signals corresponding to the successive increment in glucose concentration at $Pd_{30}Au_{70}$/C, a chronoamperometric test was carried out on a rotating disk electrode (1600 rpm) at −0.2 V (vs. Hg/HgO), which is positive enough to oxidize the glucose molecules as clearly seen from CV results. As shown in Fig. 8, once 1 mM glucose is successively injected into 0.1 mol L^{-1} NaOH solution, the current sharply increases and then decreases to relatively constant value. The current response time is very short (ca. 3 s). The corresponding calibration plot for current vs. glucose concentration is linear in the investigated rang with a slope of 2.372 μA mM^{-1}.
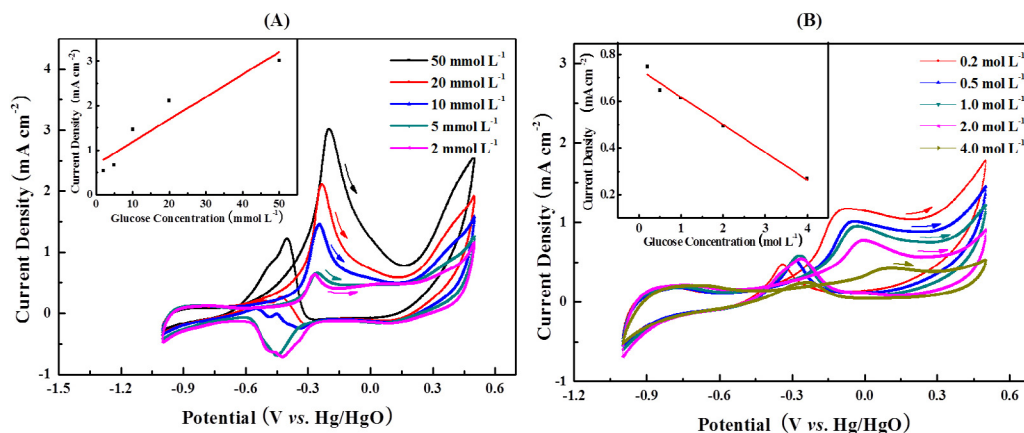

Fig. 7. Cyclic voltammograms for $Pd_{30}Au_{70}$/C catalyst in 0.1 mol L^{-1} NaOH aqueous solution containing different concentrations of glucose at 50 mV s^{-1} and at 36.5 °C. Inset is the relationship between peak current densities and glucose concentrations.
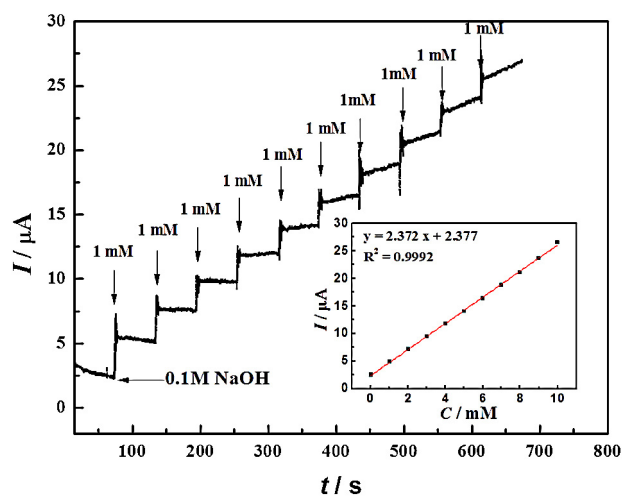
Fig. 8. Current–time record of $Pd_{30}Au_{70}/C$ catalyst fixed onto rotating disk electrode (1600 rpm) by successively injection 1 mM glucose into 0.1 M NaOH solution at a regular interval time of 60 s. Applied potential: −0.2 V. Inset is the relationship between the current density and the added glucose solution.

4. Conclusions

Pd_xAu_y/C binary catalysts were synthesized by a modified pulse microwave assisted polyol method and investigated for glucose electrooxidation and detection. The composition of Pd_xAu_y/C catalysts could be controlled and adjusted by changing the corresponding composition ratio in the precursor solutions. Pd/C mono-metallic catalyst exhibits high activity toward glucose electrooxidation but easily poisoned. The introduction of Au is vital to relieve poisoning of Pd, and the optimum $Pd_{30}Au_{70}/C$ exhibits the desirable activity to glucose oxidation as well as tolerance to the intermediate species produced from glucose electrooxidation. Pd_xAu_y binary catalysts are expecting to have potential applications for electrochemical glucose sensors or direct glucose fuel cells.

Acknowledgements

Appendix A. Supplementary data

Supplementary data associated with this article can be found, in the online version, at http://dx.doi.org/10.1016/j.apcatb.2013.12.026.

References

[1] M.L.B. Rao, R.F. Drake, J. Electrochem. Soc. 116 (1969) 334–337.
[2] U. Gebhardt, J.R. Rao, G.J. Richter, J. Appl. Electrochem. 6 (1976) 127–134.
[3] N. Mano, F. Mao, A. Heller, J. Am. Chem. Soc. 124 (2002) 12962–12963.
[4] A. Heller, Phys. Chem. Chem. Phys. 6 (2004) 209–216.
[5] D. Basu, S. Basu, Int. J. Hydrogen Energy 37 (2012) 4678–4684.
[6] D. Basu, S. Basu, Int. J. Hydrogen Energy 36 (2011) 14923–14929.
[7] D. Basu, S. Basu, Electrochim. Acta 55 (2010) 5775–5779.
[8] D. Basu, S. Sood, S. Basu, Chem. Eng. J. 228 (2013) 867–870.
[9] Y.B. Vassilyev, O.A. Khazova, N.N. Nikolaeva, J. Electroanal. Chem. 196 (1985) 105–125.
[10] S. Park, T.D. Chung, H.C. Kim, Anal. Chem. 75 (2003) 3046–3049.
[11] K.B. Kokoh, J.M. Léger, B. Beden, H. Huser, C. Lamy, Electrochim. Acta 37 (1992) 1909–1918.
[12] Y.B. Vassilyev, O.A. Khazova, N.N. Nikolaeva, J. Electroanal. Chem. 196 (1985) 127–144.
[13] L. Li, K. Scott, E.H. Yu, J. Power Sources 221 (2013) 1–5.
[14] M. Pasta, L. Hu, F.L. Mantia, Y. Cui, Electrochem. Commun. 19 (2012) 81–84.
[15] M.W. Hsiao, R.R. Adžic, E.B. Yeager, J. Electrochem. Soc. 143 (1996) 759–767.
[16] S.P. Tung, T.K. Huang, C.Y. Lee, H.T. Chiu, RSC Adv. 2 (2012) 1068–1073.
[17] Q. Li, S. Cui, X. Yan, J. Solid State Electrochem. 16 (2012) 1099–1104.
[18] Z. Liu, L. Huang, L. Zhang, H. Ma, Y. Ding, Electrochim. Acta 54 (2009) 7286–7293.
[19] Q. Wang, X. Cui, J. Chen, X. Zheng, C. Liu, T. Xue, H. Wang, Z. Jin, L. Qiao, W. Zheng, RSC Adv. 2 (2012) 6245–6249.
[20] L.M. Lu, H.B. Li, F. Qu, X.B. Zhang, G.L. Shen, R.Q. Yu, Biosens. Bioelectron. 26 (2011) 3500–3504.
[21] Y. Kuang, B.H. Wu, D. Hu, X. Zhang, J. Chen, J. Solid State Electrochem. 16 (2012) 759–766.
[22] C. Zhu, S. Guo, S. Dong, Adv. Mater. 24 (2012) 2326–2331.
[23] İ. Becerik, Turk. J. Chem. 23 (1999) 57–66.
[24] D. Basu, S. Basu, Electrochim. Acta 56 (2011) 6106–6113.
[25] H.F. Cui, J.S. Ye, X. Liu, W.D. Zhang, F.S. Sheu, Nanotechnology 17 (2006) 2334–2339.
[26] Y. Sun, H. Buck, T.E. Mallouk, Anal. Chem. 73 (2001) 1599–1604.
[27] A. Habrioux, E. Sibert, K. Servat, W. Vogel, K.B. Kokoh, N. Alonso-Vante, J. Phys. Chem. B 111 (2007) 10329–10333.
[28] Y. Yamauchi, A. Tonegawa, M. Komatsu, H. Wang, L. Wang, Y. Nemoto, N. Suzuki, K. Kuroda, J. Am. Chem. Soc. 134 (2012) 5100–5109.
[29] X. Yan, X. Ge, S. Cui, Nanoscale Res. Lett. 6 (2011) 313–319.
[30] C. Li, H. Wang, Y. Yamauchi, Chem. Eur. J. 19 (2013) 2242–2246.
[31] Z. Liu, L. Huang, L. Zhang, Ho. Ma, Y. Ding, Electrochim. Acta 54 (2009) 7286–7293.
[32] J.S. Ye, Y. Wen, W.D. Zhang, L.M. Gan, G.Q. Xu, F.S. Sheu, Electrochem. Commun. 6 (2004) 66–70.
[33] A. Brouzgou, L.L. Yan, S.Q. Song, P. Tsiakaras, Appl. Catal. B: Environ. 147 (2014) 481–489.
[34] V.S. Bagotzky, Yu.B. Vassilyev, Fuel Cells, Their Electrochemical Kinetics, Consult. Bureau, New York, 1966, pp. 77.
[35] S.B. Aoun, G.S. Bang, T. Koga, Y. Nonaka, T. Sotomura, I. Taniguchi, Electrochem. Commun. 5 (2003) 317–320.
[36] H. Wang, M. Imura, Y. Nemoto, L. Wang, H.Y. Jeong, T. Yokoshima, O. Terasaki, Y. Yamauchi, Chem. Eur. J. 18 (2012) 13142–13148.
[37] H. Wang, Y. Yamauchi, Chem. Asian J. 7 (2012) 2133–2138.
[38] H. Wang, S. Ishihara, K. Ariga, Y. Yamauchi, J. Am. Chem. Soc. 134 (2012) 10819–10821.
[39] C. Bianchini, P.K. Shen, Chem. Rev. 109 (2009) 4183–4206.
[40] S. Hermans, A. Deffernez, M. Devillers, Appl. Catal. A: Gen. 395 (2011) 19–27.
[41] S.Q. Song, Y. Wang, P.K. Shen, J. Power Sources 170 (2007) 46–49.
[42] S.Q. Song, J.C. Liu, J.Y. Shi, H. Liu, V. Maragou, Y. Wang, P. Tsiakaras, Appl. Catal. B: Environ. 103 (2011) 287–293.
[43] V. Radmilovic, H.A. Gasteiger, P.N. Ross, J. Catal. 154 (1995) 98–106.
[44] A. Nirmala Grace, K. Pandian, J. Phys. Chem. Solids 68 (2007) 2278–2285.
[45] S.B. Aoun, Z. Dursun, T. Koga, G.S. Bang, T. Sotomura, I. Taniguchi, J. Electroanal. Chem. 567 (2004) 175–183.
[46] S.Z. Cui, The electrocatalytic oxidation of D-glucose based on nanoporous gold film (Master thesis), Shandong University, 2010.
[47] I. Becerik, F. Kadirgan, Electrochim. Acta 37 (14) (1992) 2651–2657.
[48] J. Wang, G. Rivas, M. Chicharrro, J. Electroanal. Chem. 439 (1997) 55–61.
[49] M.S. Gelej, G. Rivas, Electroanalysis 10 (1998) 771–775.